

IMPERIAL COLLEGE LONDON

3RD YEAR BSC PROJECT

Investigation of the Stability of the Electron Plasma within the Gabor Lens

Chung Lim Cheung

CID: 00937227

Supervised by
Dr. Piero POSOCCO

May 7, 2017

Acknowledgements

I would like to thank my supervisor, Dr. Piero Posocco, as well as my examiner, Dr. Jürgen Pozimski for giving me this opportunity to work on the Gabor lens at Imperial College London.

I would like to further thank Dr. Jürgen Pozimski for the patient guidance, encouragement and the assistance he has provided throughout the project.

Furthermore, Dr. Piero Posocco has provided us the computer simulation for the mechanical movement of the detector for the comparison between our experimental results.

I would also like to acknowledge with much appreciation for the assistance provided by the PhD student, Toby Nonnenmacher, who was working on the Gabor lens at the same time.

Last but not least, many thanks go to my lab partner, Ben Elliott, for working alongside me and providing continuous support and encouragement.

Abstract

A 16-segmented detector was located at one end of the Gabor lens to detect the expulsion of positive ions and electrons in order to investigate the conditions for unstable plasma to occur. The plasma in the Gabor lens were operated in different regimes at varying high voltage at the anode and magnetic field from the solenoid. The voltage regime was found to be the most stable and favourable for focusing using results from the Fourier transform of the direct ion current measurements. The theory of the production of the positive ions and electrons was verified by the agreement between the experimental results and the computer simulation for the mechanical movement of the detector. No correlations were observed between any features such as the magnetic field required for the start-up of the plasma and the high voltage supplied to the anode. The correlations could have been suppressed and masked by the increase in temperature due to the heating from the current in the solenoid. The plateau regions were caused by the expulsion of electrons inside the plasma as the electron density increased with the magnetic field. Hence it would be most stable just before the start of the plateau region as the highest density of electrons would be confined inside the plasma with negligible electron expulsion.

Contents

1	Introduction	4
1.1	History of the lens	4
1.2	Application of the lens	4
1.3	Experimental Set-up	5
1.4	Motivation and Aim	5
2	Gabor Lens Background Theory	7
2.1	Focal Length	7
2.2	Property of the Plasma	7
3	Direct Ion Current	9
3.1	Theory	9
3.2	Method	9
3.3	Results	10
4	Fourier Spectrum	13
4.1	Theory	13
4.2	Method	13
4.3	Results	13
4.3.1	Comparison with and without Faraday Cage	13
4.3.2	Comparisons between Different Regimes	13
5	Mechanical Movement of the Detector	16
5.1	Theory	16
5.2	Method	16
5.3	Results and Comparison	16
5.3.1	Concentric Circles	16
5.3.2	Sectors	17
6	Base Voltage Measurement	18
6.1	Theory	18
6.2	Method	18
6.3	Results	18
6.3.1	Variation in Magnetic Field	18
6.3.2	Variation in Temperature	19
6.3.3	Variation in Current in the High Voltage supply	20
7	Problems Encountered	21
8	Conclusion and Outlook	22

1 Introduction

1.1 History of the lens

The Gabor lens, often referred to as the plasma lens or space-charge lens, was proposed by Dennis Gabor in 1947 ^[1]. It is a very powerful focusing lens for particle beams using a non-neutral plasma. The plasma is confined radially by a uniform axial magnetic field, which is produced by supplying a current to the solenoid wound around the lens. It is confined longitudinally by an electrostatic field, which is produced by supplying a high voltage to the cylindrical anode shown in Figure 1. The magnetic field also prevents most of the electrons from reaching the anode while the anode potential is below a certain threshold value.

There are 3 main mechanisms used to fill the lens with electrons ^[2]:

1. Electron production by collisional ionisation between beam ions and residual gas
2. Electron production by a hot cathode (originally proposed by Gabor)
3. Electron production by a gas discharge depending on the pressure

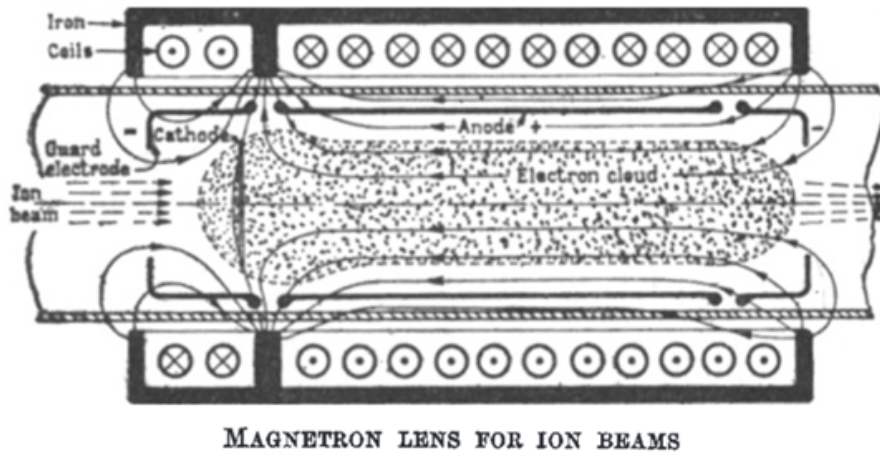


Figure 1: Original design of the Gabor lens in 1947

The Gabor lens had been continuously investigated since 1947, including the testing of different geometry and the increasing of the anode voltage to increase the stability of the lens in 1988 by Palkovic ^[3]. Reiser also compared the efficiency between the Gabor lens and electrostatic quadrupole (ESQ) doublet and found that the Gabor lens was significantly more efficient if the trapping efficiency is close to the theoretical Brillouin limit in 1989 ^[4]. Palkovic investigated the use of the Gabor lens for focusing negative ion beam in 1989, but it was found not to be feasible because the minimum magnetic field required to confine heavy positively charged ion plasma was 6 kG ^[5]. Klein attempted to use the Gabor lens to focus plasma into non-neutral cloud of inertial electrostatic confinement fusion in 2009, but then experienced technical difficulty on the fundamental design of the MIX ^[6].

1.2 Application of the lens

Radiation therapy is the medical use of ionizing radiation to treat cancer ^[7]. In order to maximise the radiation dosage to the tumour and minimise the dosage to the surrounding tissue, hadron therapy is much more favourable than photon such as X-ray for deep seated tumours. However, conventional radiotherapy are expensive, hence there are only 22 proton therapy centres across the globe and they are not as widespread compared with conventional X-ray ^[8].

Recent experiments showed that laser driven proton accelerators could potentially replace conventional accelerators, and Pozimski proposed a cheaper and more compact solution for hadron therapy using the Gabor lens in 2012 ^[9]. The reasons why the Gabor lens is a more affordable solution, is that the Gabor lens requires a field less than 1 Tesla to capture the Carbon 6^+ beam, enabling the use of conventional conduction magnets, whereas a solenoid capture system requires 20 Tesla ^[10]. Secondly, less beam bending and radiation shielding is required since the source can be mounted directly on a gantry.

3 Gabor lenses are required for a full therapy solution. The first lens captures the diverging ion beam, the second lens allows energy separation, and the third prepares the beam as such that it is suitable for the treatment ^[9].

However, the maximum energy achieved by the laser driven proton accelerator is currently around 80 MeV, whereas the energy required for the hadron therapy treatment is around 250 MeV, so it is not yet sufficient for medical purposes ^[10].

1.3 Experimental Set-up

To further investigate the property of the lens for medical applications, Imperial College London has built a Gabor lens. A photograph and the internal structure of the Imperial College (IC) Gabor lens are shown on figure 2 ^[11].

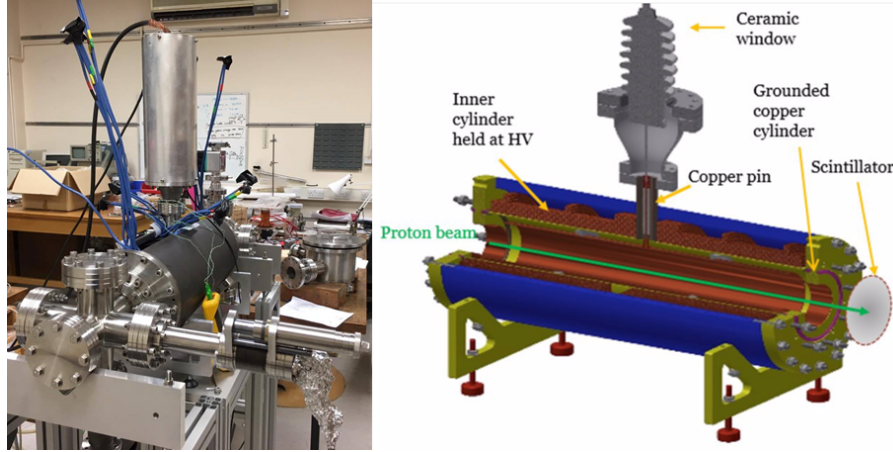


Figure 2: A photograph and the internal structure of the IC Gabor lens

The combination of the internal resistance of the high voltage (HV) supply and the resistance of the cylindrical electrode forms a potential divider. A high voltage was supplied to the cylindrical electrode via the copper pin and held in place by the ceramic window, according to the effective resistance of the cylindrical electrode and the pre-set high voltage on the HV supply.

The combination of the cylindrical electrode and the grounded electrode at both ends confined the electron plasma longitudinally and expelled the positive ions. The solenoid producing the magnetic field for the radial confinement is not shown in Figure 2.

The chamber was depressurised down to 10^{-7} millibar using a vacuum pump. The residual gas remaining in the chamber was ionised by cosmic rays initially, freeing the outer-shell electrons from the positively charged nuclei. The free electrons then further ionised the residual gas via collisions, created an avalanche production of electrons. The electrons then diffused throughout the chamber, forming a uniformly distributed plasma.

An adjustable 16-segment detector was placed at one end of the chamber, detecting the expulsion of positive ions and electrons from the plasma, measuring current. The signals were then fed to a 4-channel Tektronix DPO 3014 Digital Phosphor Oscilloscope with an internal resistance of $1\text{ M}\Omega$ via the junction box, thus 4 segments were combined into 1 channel on the oscilloscope. This was done in either a concentric circle or sector arrangement shown in figure 3.



Figure 3: A photograph of the 16-segment detector in different arrangements: sector (middle), concentric circle (right)

In order to reduce the noise in the data, a Faraday cage was made from a tin can and the junction box was placed inside. A Faraday cage is a hollow conductor that redistributes the charges on the exterior of the cage, canceling out any electrostatic field or radiation within the interior.

1.4 Motivation and Aim

The lens was tested at the Surrey ion beam centre in 2015 with a 1 MeV proton pencil beam. The output proton beam was displayed as a light signal on scintillator at the focal point and photographs of the light were taken by a charge-coupled device camera ^[12]. At low current, the pencil beam remained the same as if the lens was off. However, as the current increased, the magnetic field increased, and the beam was not focused instead

it was converted into a ring, and the size of the ring increased with current as shown in Figure 4 ^[10]. This strongly indicates the existence of an instability inside the lens.

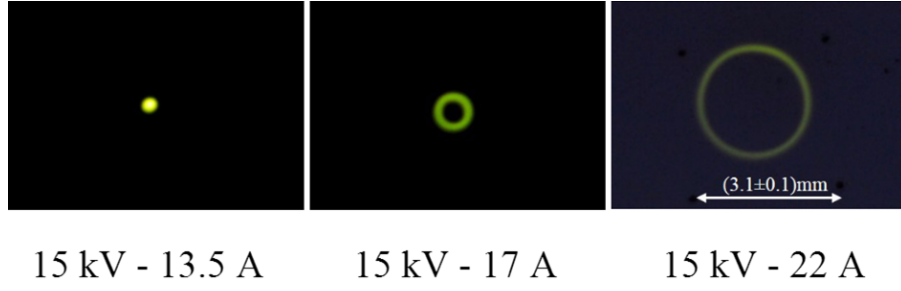


Figure 4: A series of photographs of the ring with increasing magnetic field

The aim of the project was to investigate the stability of the plasma and the condition for instability to occur inside the plasma. Similar phenomena were observed by Neuner in 2000 ^[13], which was a result of a high-current discharge causing an under- or over- focusing. However, no electron discharge was present in the experiment. The non-uniform magnetic field due to the obstruction of the feed-through of the HV could potentially be the cause of the ring. This has been solved by adding correction coils to the solenoid to reduce the depression of the magnetic field. The pressure of the residual gas was also at 10^{-6} milibar, having a high overall collision rate could lead to plasma oscillations, this has been solved by improving the pressure down to 10^{-7} milibar.

2 Gabor Lens Background Theory

2.1 Focal Length

The focusing force on positive ion beams is produced by the space charge of the electron cloud inside the chamber. From solving the equation of motion for the electrons inside the plasma using the momentum equation for electron fluid in Equation 1 and Gauss's law, the focal length can be evaluated.

$$m_e n_e \frac{dV_e}{dt} = -en_e(\underline{E} + \underline{V}_e \times \underline{B}) - \underline{\nabla} P_e \quad (1)$$

where $en_e(\underline{E} + \underline{V}_e \times \underline{B})$ is the Lorentz force acting on the electron from the electromagnetic field inside the lens and $\underline{\nabla} P_e$ is the pressure gradient. Equation 1 neglects any effects of collisions.

The maximum radial electron density n_r that can be confined by the axial magnetic field $\underline{B} = B_0 \hat{z}$ can be calculated by solving the equation with certain boundary conditions and is given by the Brillouin flow ^[14]:

$$n_r = \frac{\epsilon_0}{2m_e} B^2 \quad (2)$$

The maximum longitudinal electron densities n_l that can be confined by the electrostatic field can be calculated by the radius r_c and the potential V_c of the cylindrical electrode ^[14].

$$n_l = \frac{4\epsilon_0 V_c}{er_c^2} \quad (3)$$

By equating the radial and longitudinal electron density i.e. $n_r = n_l$, the threshold potential can be calculated for the prevention of electrons flowing to the anode by the magnetic field.

$$V_c = \frac{er_c^2}{8m_e} B^2 \quad (4)$$

Considering a positive ion with mass m_i with charge q enters the lens with longitudinal velocity \underline{v} experiences a focusing force \underline{F}_f ^[14].

$$\underline{F}_f = m_i \underline{a} = -\frac{qn_r e}{2\epsilon_0 v^2} \underline{r} \quad (5)$$

By substituting the maximum radial electron density n_r , the focusing force can be rewritten as

$$\underline{F}_f = -\frac{em_i}{8m_e} \frac{B^2}{U_B} \underline{r} \quad (6)$$

where $U_B = (\frac{m_i v^2}{2q})$ is the total accelerating potential of the ions.

Hence the focal length f of a Gabor lens can be evaluated as ^[14]

$$\frac{1}{f} = \frac{e}{8m_e} \frac{B^2}{U_B} l \quad (7)$$

where l is the effective lens length.

Equation 7 shows that the focal length of a Gabor lens is proportional to the energy of the ion, whereas the focal length of an ESQ is proportional to the root of the energy of the ion, showing that the Gabor lens has a greater focusing efficiency ^[14].

2.2 Property of the Plasma

When an external magnetic field is acting on a charged particle, the magnetic moment of the particle precesses about the axis of the magnetic field. The angular frequency of the precession is known as the Larmor frequency. The Larmor frequency of an electron Ω_e can be calculated using Equation 8.

$$\Omega_e = \frac{|eB|}{m_e} \quad (8)$$

Considering a layer of electrons being displaced, disrupting the uniform distribution of the plasma. The charge separation generates an electric field, and electrons moves to restore the charge imbalance, generating a plasma oscillation. A typical electrostatic oscillations frequency corresponds to the plasma frequency ω_p .

$$\omega_p = \left(\frac{n_e e^2}{\epsilon_0 m_e} \right)^{\frac{1}{2}} \quad (9)$$

The collision time τ_c between electrons and residual gas particles can be evaluated using the mean free path λ_{mfp} and the velocity of the electrons $\underline{v_e}$ under the assumption that the velocity of the residual gas particle is negligibly slow when compared with the electron velocity, i.e. stationary.

$$\tau_c = \frac{\lambda_{mfp}}{|\underline{v_e}|} \quad (10)$$

Number of gyrations completed by the electron per collision $\Omega_e \tau_c$ can then be calculated.

3 Direct Ion Current

3.1 Theory

The residual gas is ionised through collisional ionisation, separating the electrons from the positive ions. From the nature of the charge of the cylindrical electrode (positive), the electrons are confined inside the chamber and the positive ions are expelled out of the lens, hence the current measured at the detector is mostly that of the ions.

$$I_d \propto n_e n_{RGA} v_e \sigma \quad (11)$$

The current measured at the detector is proportional to the velocity v_e and density n_e of the electron, density of the residual gas atoms n_{RGA} and the cross section of the collision σ between the two.

However, those electrons at the Maxwell tails that have higher energy than the longitudinal potential leave the lens longitudinally. Additionally, as the electrons fill up the lens, the potential that confines the plasma longitudinally drops due to the electric field of the electrons. Hence the number of electrons measured at the detector becomes comparable to the number of ions expelled by the plasma when the lens is full.

As the magnetic field increases, the radius of the plasma decreases, resulting in a higher electron density. This consequently increases the electrostatic potential energy of the electrons, if the potential energy is higher than the potential that confines them, this results in electron expulsion, hollowing out regions of the electron plasma.

The electrons also flow towards the anode, leaving the lens radially. This is generally prevented by the magnetic field. However, some number of electrons diffuse outwards from the high density electron cloud towards the anode, and some drifts outwards via the $\underline{E} \times \underline{B}$ drift, resulting in a small current flowing between the plasma and the anode.

There are 3 main regimes that the plasma can operate in:

1. The voltage regime (VR)
2. The limited current regime (LCR)
3. The non-limited current regime (NLCR)

The plasma operates in the voltage regime when a negligible number of electrons flow from the electron cloud to the anode, thus the electrons are not depleted and a negligible current flows in the cylindrical electrode and in the HV supply.

The plasma operates in the current regime when the anode is connected to the plasma electrically, such that there is a constant flow of electrons from the plasma to the anode, thus a constant depletion of electrons from the plasma and a significant current flow in the HV supply circuit. As the electrons flow to the anode in a helical path due to the magnetic field, they have a high probability of colliding with residual gas atoms and ionising them. The electrons from the residual gas atoms then diffuse back into the plasma to replenish the depletion of electrons.

The current regime occurs when the breakdown voltage is reached by the voltage between the plasma and the anode, i.e. the insulator becomes electrically conductive. This behaviour can be described by the Paschen curve, a curve that gives the breakdown voltage between two electrodes as a function of pressure and gap length, shown in Figure 5.

In order to investigate which region of the Paschen curve the plasma is operated in, the path length between the two electrodes is required. If the number of gyrations completed by the electron per collision is much smaller than 1, i.e. $\Omega_e \tau_c \ll 1$, the path length is simply the geometrical distance between the plasma and the anode. If the number of gyration completed by the electron per collision is much greater than 1, i.e. $\Omega_e \tau_c \gg 1$, the magnetic field affects the flow of electrons, and the path length is much greater than the geometrical distance due to the helical path of the electron instead of a straight path, the exact path length is too complicated to compute since many different factors of collisions are needed to be taken into account.

3.2 Method

The offset voltage was measured from the current flowing in the detector using the oscilloscope with an internal resistance of $1M\Omega$. The offset voltage was measured at a sampling rate of 25 million for 4 milliseconds. The scale on the oscilloscope was set to 5 mV for no plasma inside the lens, and 2 V for different regimes. The pre-set base HV was kept constant at 10 kV in this section. In order to operate from the voltage to current regime, the current that flows in the solenoid was increased from 22.1 A to 28.2 A to increase the magnetic field. By manually decreasing the current in the HV supply from 1.41 mA to 0.21 mA, the plasma operated in the limited current regime instead of the non-limited current regime.

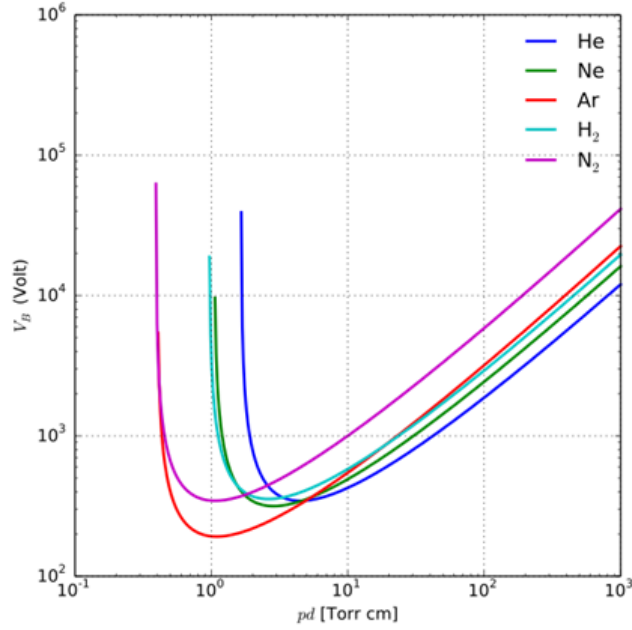


Figure 5: A curve that gives the breakdown voltage between two electrodes as a function of pressure and gap length

3.3 Results

The parameters and results for different regimes are shown in Table 1, and the graphs that show how the offset voltages varied with time in different regimes are shown in Figures 6, 7 and 8.

Parameters	VR	LCR	NLCR
Pre-set Voltage / kV	10.0	10.0	10.0
Anode Voltage / kV	10.0	7.4	7.12
HV current / mA	0.01	0.21	1.41
Effective Resistane / M Ω	100.0	35.2	5.0
Pressure / 10 ⁻⁶ mbar	1.62	8.25	29.8
Pressure ratio to VR	1.0	5.1	18.4
Offset voltage / kV	3	10	18
Offset voltage ratio to VR	1.0	3.3	6.0

Table 1: Different parameters and results in different regimes

The offset voltage in Figure 6 was 0 V, showing that when there was no plasma, no positive ions or electrons were produced, hence no positive ions or electrons were expelled. This also shows that the range of the offset voltage was dependent on the scale on the oscilloscope as the range in 5 mV was significantly less compared with 2 V in Figures 7, 8, 9.

The internal resistance of the HV supply was dependent on the current passing through the supply. In the voltage regime where negligible amount of electrons flow from the plasma to the anode, negligible current was observed on the HV supply, thus the internal resistance was negligible. Due to the fact that the set-up acts as a potential divider, the anode received the entirety of the base voltage of 10kV from the HV supply, strongly expelling the positive ions and confining the electrons inside the chamber.

This indicated the lifetime of the positive ions produced by ionisations was short in the chamber, hence the Debye length was large. Hence this regime had the largest focusing power for the positive ion beam which is favourable for the purpose of the lens.

As the magnetic field increased, the lens was operated in the current regime. As the plasma was operated in the limited- and non-limited current regime, the offset voltage increased from 3 V up to 10 V and 18 V respectively, agreeing with the theory. This was caused by the extra ionisations that occurred when the electrons flowed from the plasma to the anode helically, producing electrons that replenished the depleted electrons, and expelling the positive ions produced, increasing the current measured at the detector, hence increasing the offset voltage on the oscilloscope.

The electrons that flowed from the plasma to the anode increased the current in the HV supply circuit, thus the internal resistance of the HV supply increased. This resulted in the anode receiving a smaller voltage due to the potential divider set-up. In the limited current regime, the current observed at the HV supply was increased

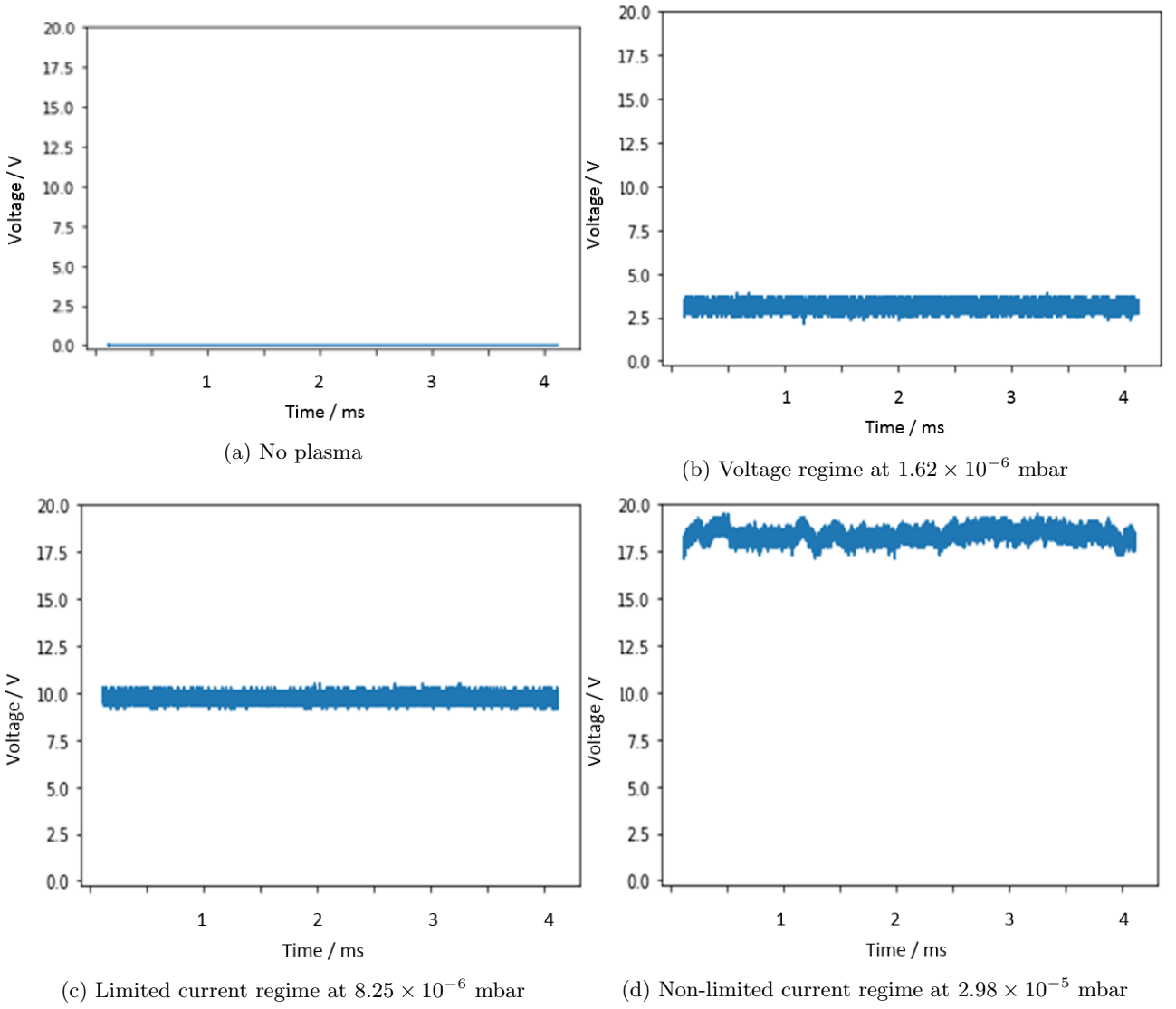


Figure 6: Graphs that show how the offset voltage varied with time in different regimes in channel 1

up to 0.21 mA, resulting in a lower HV of 7.4 kV received by the anode. The expulsion of the positive ions were weaker compared with the voltage regime, increasing the number of positive ions remaining inside the chamber. Hence this led to an increase in pressure from 1.62×10^{-6} mbar to 8.25×10^{-6} mbar due to weaker expulsion of positive ions and the Debye length decreased, thus the current regime is less favourable for the purpose of focusing.

The current reached 1.41 mA in the non-limited current regime, resulting in an even lower HV of 7.12 kV received by the anode. The even weaker expulsion from the anode further increased the number of positive ions remaining inside the plasma, increasing the pressure from 8.25×10^{-6} mbar to 2.98×10^{-5} mbar.

The pressuremeter could not distinguish between positive ions and the residual gas atoms, hence the combination of the two made up the measured pressure. From Equation 11, if the increase in pressure was solely caused by the increase in the number of positive ions remaining inside the plasma from regime to regime, then the current measured at the detector should have remained constant. Interpreting the values and ratios of pressures and measured voltage in different regimes in Table 1, it was indicated that the increase in pressure was not solely caused by more positive ions remaining in the plasma, hence the density of the residual gas atoms increased. It showed that 60% and 34% of the pressure increased was due to the increase in residual gas atoms using the result. This was caused by the increase in the number of positive ions remaining inside the plasma due to the decrease in the anode voltage. A potential interpretation of this result could be that when a positive ion flows to the casing of the lens which acts as ground, it interacts and releases residual gas atom from the surface of the casing, increasing the density of residual gas atoms inside the chamber.

As the magnetic field increased, the electron density inside the plasma increased, and the stability of the offset voltage decreased as shown in the figures. This was caused by the longitudinal expulsion of the electrons inside the plasma. As the electron density increased, the longitudinal potential that confined the electrons dropped, hence more electrons were able to escape, causing a fluctuation in the current measured at the detector.

The magnetic field was 0.024 T, the mean free path of an electron in a residual gas pressure of 10^{-6} mbar

was 5.9×10^5 m ^[15]. The energy of the electrons in the plasma was estimated to be 100 eV, hence the electrons completed 5.9×10^8 gyrations before a collision, which was much greater than 1, thus the path length was strongly affected by the magnetic field and it was much greater than the geometrical distance and the exact path length could not be determined from this calculation.

The voltage between the two electrodes was kept constant, but when the magnetic field was gradually increased, the breakdown voltage was reached and the plasma entered the current regime. As the magnetic field increased, the radius of the plasma reduced and the helical path length of the electrons between the plasma and the anode increased, hence the voltage required for the breakdown must decrease with path length i.e. negative gradient, thus the path length could be estimated from the Paschen curve.

Assuming the conditions in the voltage regime was on the boundary of the breakdown voltage, i.e. 10 kV, and the pressure was at 1.62×10^{-6} mbar, the path length would be estimated to be 3.3 km using Figure 9, compared to the geometrical distance in the magnitude of centimeters.

4 Fourier Spectrum

4.1 Theory

Any oscillation or rotation of the plasma inside the lens have a characteristic frequency. When the offset voltage in the time domain is decomposed into its frequency components by a Fourier transform, significant peaks would be present in the Fourier spectrum at its characteristic frequency if there are any oscillations or instabilities.

4.2 Method

The offset voltage data was recorded by the oscilloscope with the same sampling rate and duration as in Section 3. The junction box was placed inside and outside the tin can without a plasma for comparisons to test the sufficiency of the tin can acting as a Faraday cage. The scale was down to 2 mV as opposed to 5 V in Section 3, since the offset voltage was minuscule compared to those with a plasma.

The data including the offset voltages recorded at different regimes in Section 3 was then Fourier transformed using Real-value Fast Fourier Transform function on Python.

4.3 Results

The frequency range of the spectrum depended on the sampling rate of the oscilloscope. With a sampling rate of 25 million per second, the Fourier spectrum had a range up to 12.5 MHz. Both the Larmor frequency of the electron and the plasma frequency were in the range of GHz, hence both of the frequencies were not observable in the spectrum.

4.3.1 Comparison with and without Faraday Cage

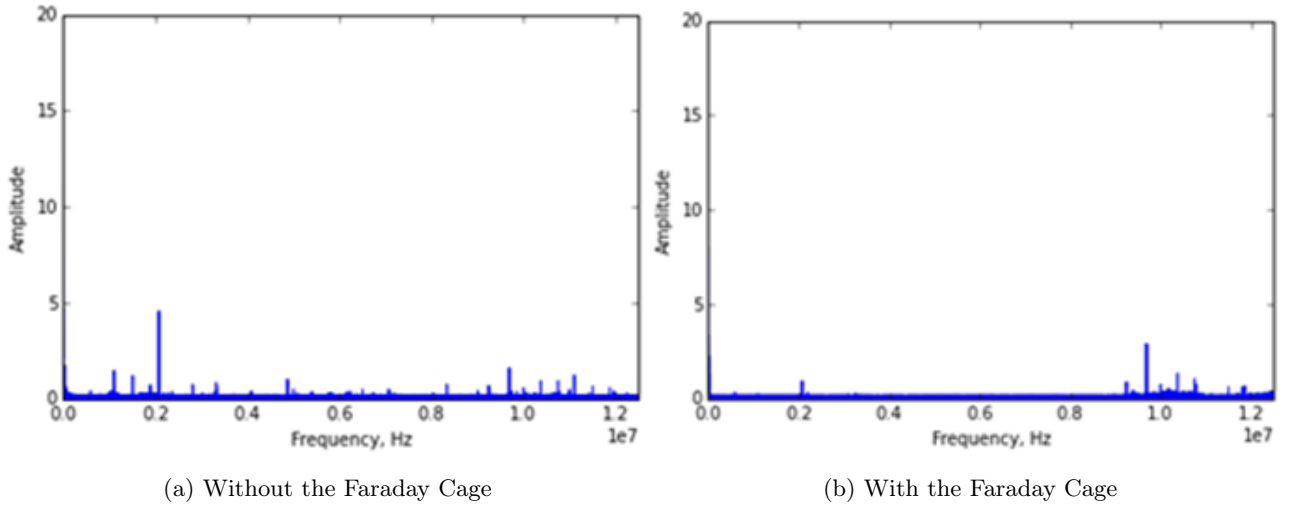


Figure 7: A Fourier spectrum of the offset voltage

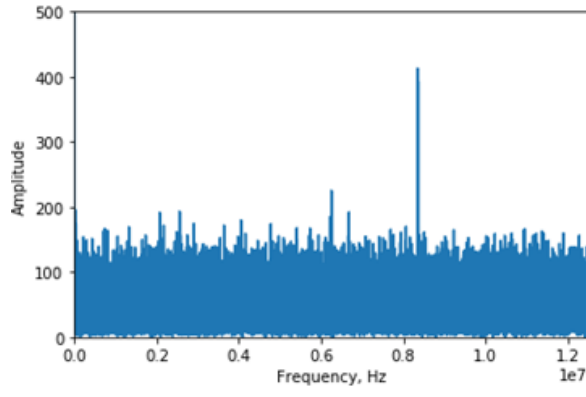
In Figure 10(b), the junction box was placed inside the Faraday cage and it had significantly reduced the number of peaks from 0 to 90 MHz compared to Figure 10(a), and a small number of peaks remained at the higher end of the spectrum. The remaining peaks could be caused by the internal frequency of the current or HV supply, showing that the tin can was working sufficiently as a Faraday cage.

4.3.2 Comparisons between Different Regimes

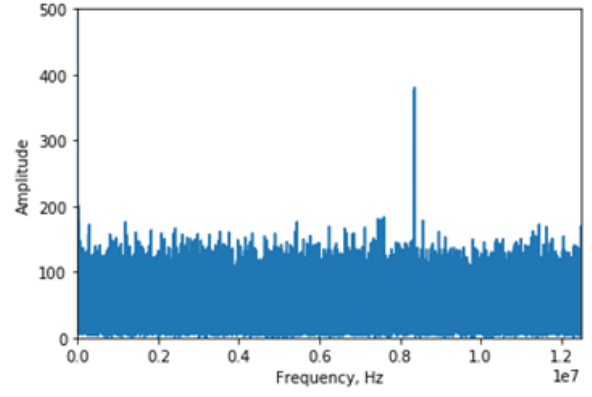
The scale on the oscilloscope was increased from 5 mV to 2 V from 4.3.1 to 4.3.2. By comparing the two, it was clear that the background noise observed in Figure 10 was caused by the digitiser and the amplitude of the noise increased with the scaling on the oscilloscope.

It appeared that no significant peaks were observed in all three figures, hence it implied that the plasma were stable in all three regimes. However, significant peaks were observed in Figure 12 as the range reduced to 1.2 kHz.

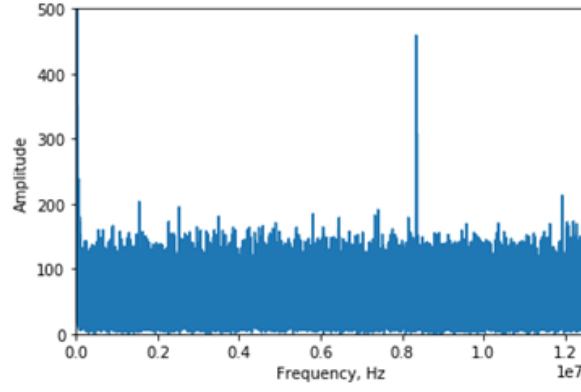
There is a correlation between the instability in the offset voltage and the amplitude of the peaks in the reduced range Fourier spectrum. The most stable regime was the voltage regime, and the relative amplitude of the significant peak was 300,000 units. The least stable regime was the non-limited current regime, and the relative amplitude of the significant peak was up to 1.8 million units.



(a) Voltage regime

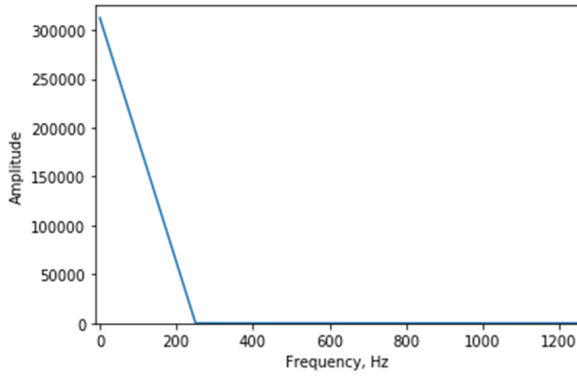


(b) Limited current regime

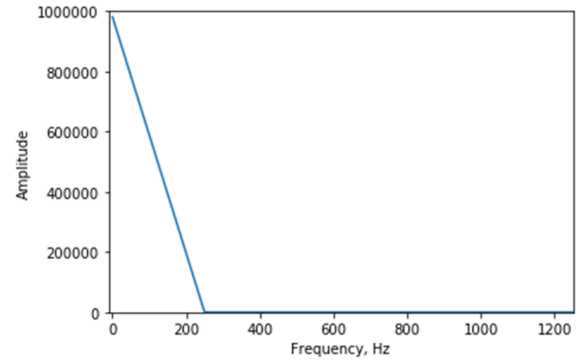


(c) Non-limited current regime

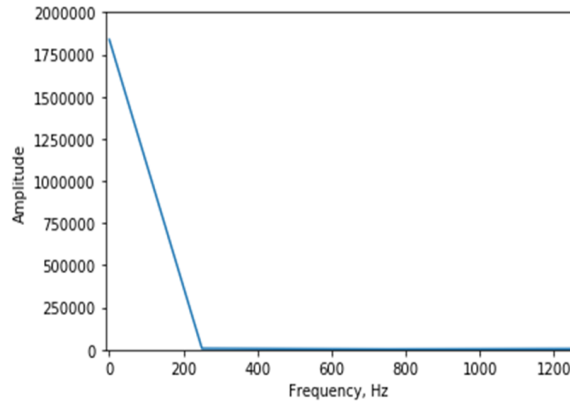
Figure 8: Fourier spectra of the offset voltage in different regimes



(a) Voltage regime



(b) Limited current regime



(c) Non-limited current regime

Figure 9: Reduced range Fourier spectra of the offset voltage in different regimes

The exact cause of this significant peak is yet to be determined, whether or not it was caused by the plasma or the power supply. A longer recording duration is required in order to observe the full period of the oscillation and locate the exact characteristic frequency, since the resolution in the frequency spectrum was only up to 250 Hz for the recording duration of 4 milliseconds.

5 Mechanical Movement of the Detector

5.1 Theory

As the residual gas atoms are ionised, the positive ions gain velocity in both the longitudinal and radial direction. The radial velocity arises from the ions accelerating towards the zero potential at the axis from the voltage drop. Assuming the location of collisional ionisation is homogeneous in the radial direction, the radial velocity is a rectangular function with respect to the radius of the plasma. The longitudinal velocity arises from the ions accelerating towards the grounded electrode. The positive ions are easily stripped off the electrons in between the cylindrical electrode and the grounded electrode, hence collisional ionisation is more likely to occur between the two electrodes, thus the longitudinal velocity is a narrow Gaussian function with respect to the longitudinal distance on the axis. The convolution of the two forms a bell-shaped distribution and the ions leave the plasma in a cone.

In the concentric circle arrangement, depending on the radii of the detector and the plasma, two distinct distributions would be observed across the channels. If the radii of the circle is smaller than the size of the plasma, the distribution would be bell-shaped. If the radii of the circle is larger than the size of the plasma, the distribution would be inverted. This can be demonstrated in the series of diagrams below:

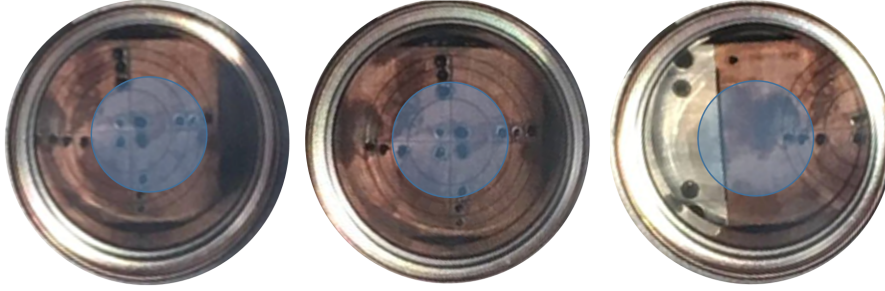


Figure 10: A series of diagrams showing how the movement of the detector varies the offset voltage, where the blue circle is representing the plasma

Channels 1 and 2 receive maximum number of positive ions when the detector is in the centre, and channels 3 and 4 receive negligible amount. As the detector moves left or right, channels 1 and 2 receive fewer, whereas channels 3 and 4 receive more. This is the explanation for why the distribution of voltage received is different depending on the radii of the detector and the size of the plasma.

In the sector arrangement, all 4 channels receive the same number of positive ions if the detector is perfectly centred. The two sectors on the left and right receive the same amount of positive ions as the detector moves if the detector is not slanted in the chamber.

5.2 Method

Initially, the 4 channels on the oscilloscope were the 4 concentric circles on the detector. The offset voltages on each of the channels were recorded for every 2 mm shift of the detector from right to left inside the chamber.

Using the theory of the escape cone of the positive ions, a simulation code was written that calculates the offset voltage in different channels at different detector position with variable radius of the cone ^[16]. The cone theory was verified by comparing the experimental data and the simulation.

By reconnecting the 4 segments in the same sector into one channel, the mechanical movement of the detector in sector arrangement was measured. Both the current of the solenoid and the HV of the cylindrical electrode was kept constant at 20 A and 10 kV in this experiment, and the plasma was initially operating in the voltage regime.

5.3 Results and Comparison

5.3.1 Concentric Circles

By comparing Figures 11 (a) and (b), it shows that the experimental data mostly agreed with the computer simulation, hence the cone theory was verified. The main difference was that the offset voltages measured by channels 3 and 4 were 540 mV and 270 mV respectively in the centre, whereas both of the channels were zero in the simulation. This showed that the detector was not perfectly centred, but shifted vertically higher or lower from the centre, allowing channels 3 and 4 to receive a fraction of the positive ions.

The plasma also operated in the current regime when the detector was moved more than 20 mm to the left i.e. detector position < -20 mm, which was not expected by the simulation. The detector could potentially be charged by the positive ions, and sparked to the grounded casing of the lens as the detector moved closer to the casing, causing the plasma to operate in the current regime.

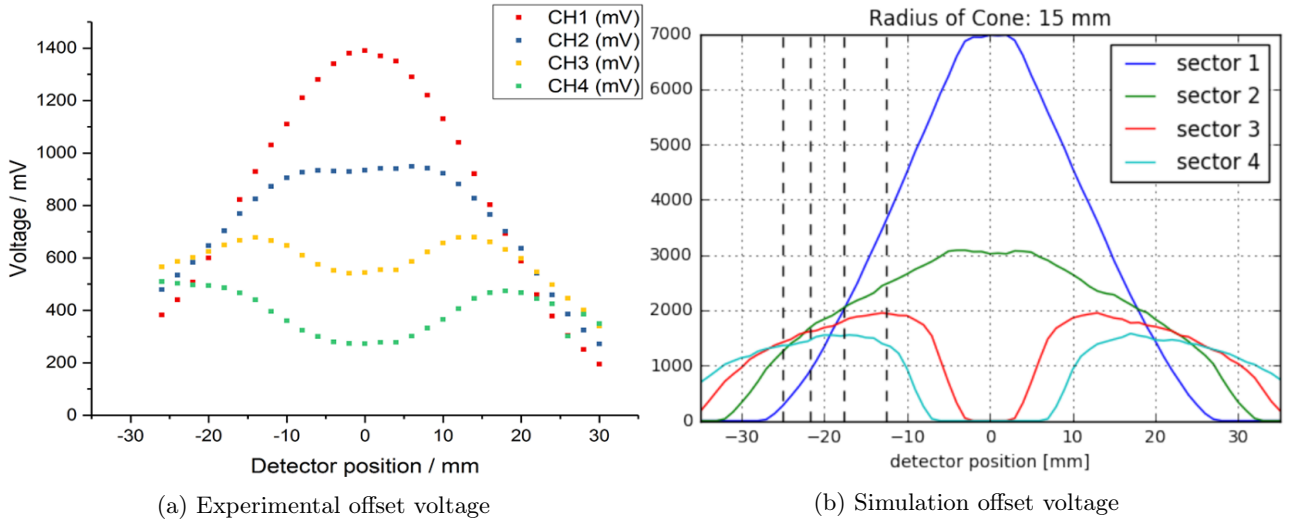


Figure 11: Graphs showing how the experimental and simulation offset voltages at each concentric circles varied with the position of the detector

5.3.2 Sectors

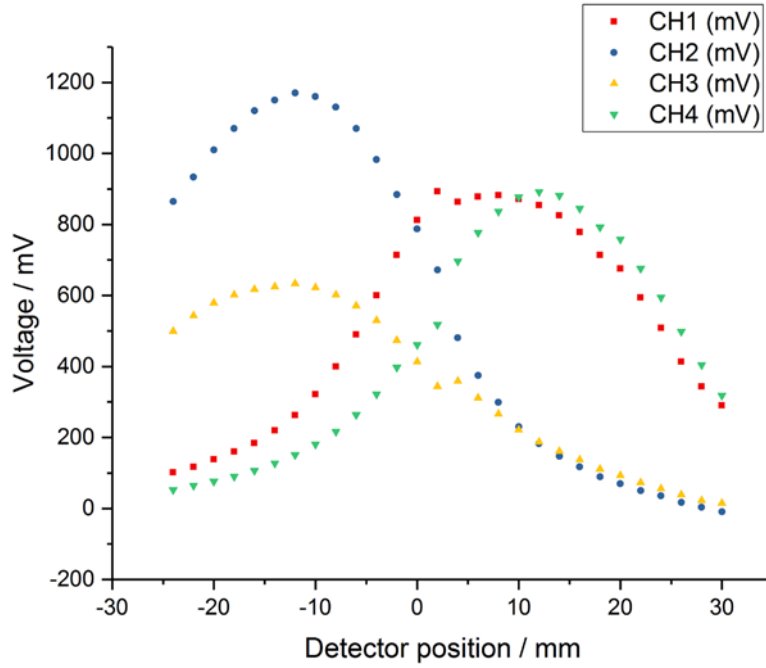


Figure 12: A graph showing how the offset voltage varied with the position of the detector in the sector arrangement

From observing the values of each channels at the centre, it clearly indicates that the detector was not perfectly centred as each channel's offset voltages differed. The graph was also not symmetric at the zero point, hence showing that the detector was not only not perfectly centred, but also slanted.

6 Base Voltage Measurement

6.1 Theory

By fixing the pre-set HV in the cylindrical electrode, and varying the magnetic field, temperature and the current in the HV supply individually, different effects and features of the plasma can be observed from the offset voltage on the oscilloscope.

Since driving a current in the solenoid to create a magnetic field inside the chamber unavoidably heats up the lens and the plasma in the absence of a cooler, variation of the temperature was investigated in order to observe the effect it has on the data collected for a long period of time.

6.2 Method

The offset voltages for each channel were measured on the oscilloscope for every increment of the current for the magnetic field from the start-up of the plasma to the plasma operating in the current regime. Since this data collection process required a constant flow of current in the solenoid for the duration of the data set, the temperature increased around 10°C - 25°C for each data set depending on the duration. In order to keep the temperature approximately constant for each data set for comparisons, all the power supplies were turned off after each set to allow the lens to cool down below 30°C before the next data set was measured. Base voltage measurements were done for 8 kV, 10 kV, 12 kV, 14 kV, 16 kV, and 20 kV, and the detector was placed in the centre.

In order to measure a data set at a higher temperature, another set at 20 kV was measured again right after the first one. The starting temperatures of the two data sets were 22.2°C and 38.6°C with starting pressures of 5.33×10^{-7} mbar and 6.76×10^{-7} mbar.

The variation in the current on the HV supply was measured in the limited current regime. This was done by increasing the magnetic field until the plasma operated in the current regime. The pre-set current on the HV supply was reduced down to 0.01 mA, the smallest possible current, and the offset voltage was measured for every increment of the current on the HV supply until it reaches the non-limited current regime.

6.3 Results

6.3.1 Variation in Magnetic Field

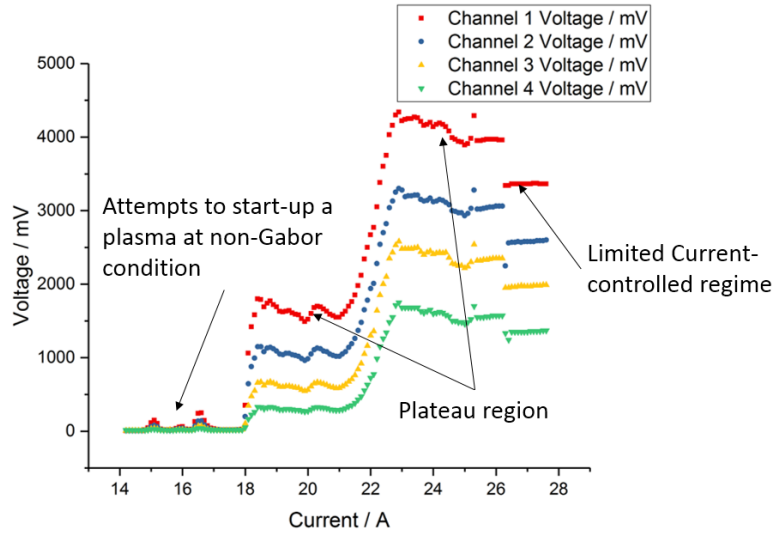


Figure 13: A graph showing how the offset voltage varied with the magnetic field produced by the current at 12 kV with annotations of the features

These base voltage measurements showed different features of the plasma at different magnetic field. The rapid rises in the voltage at various currents were observed in all the data sets. However, in some of the base voltages such as 12 kV, had small peaks before the rapid rise. These were failed attempts to form a plasma in the chamber at non-Gabor conditions where the parameters were not suitable and the electrons were not homogeneously distributed over the entire lens volume.

The rapid rise in the offset voltage indicated the formation of a plasma inside the lens where the positive ions were expelled from the electron plasma. The plateau regions were observed after the rapid increase in the offset voltages at 18 A and 23 A.

These plateau regions were caused by the expulsion of electrons inside the plasma. As the electrons filled up the lens, the potential that confined the electrons longitudinally dropped, hence more electrons at the Maxwell tail had higher energy than the longitudinal potential, thus more electrons escaped longitudinally, decreasing the current measured at the detector because the electrons and the ions were oppositely charged. Hence the lens is most stable and focusing at the peak of the rapid rise, before any electron expulsion that decreases the electron density in the plateau region.

The existence of the second rapid rise and the plateau region could not be explained using this theory because the voltage should either have remained constant or decreased due to the expulsion of electrons. The second plateau region could potentially be caused by the temperature and pressure increase due to the heating from the solenoid, hollowing regions of the electron plasma. This could be verified by installing a water-colling system to the lens to maintain the temperature of the lens.

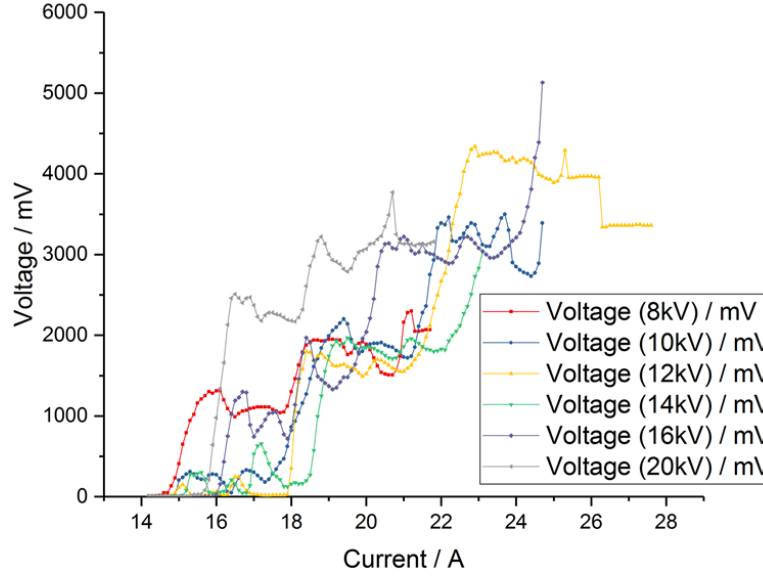


Figure 14: A graph showing how the offset voltages varied with the magnetic field produced by the current at different base voltage

Figure 23 shows that there was no correlation between the magnetic field required for the formation of the plasma and entering the current regime, offset voltage of the plateau and the base voltage of the anode. This result was unexpected because the base voltage should have had an effect to the properties of the plasma. The offset voltage of the plateau region should have been similar or proportional to the base voltage supplied since it controlled the longitudinal electron density allowed inside the plasma. The correlation could have been masked by the effect of change in temperature, hence the effect of the change in base voltages was not observed.

6.3.2 Variation in Temperature

The offset voltage at 38.6°C followed a similar trend to the one measured at 22.2°C. Unexpectedly, the one at the higher starting temperature (blue), measured a lower offset voltage than the one at the lower starting temperature (red), shown on Figure 24.

The scattering, change of the transverse momentum of an electron traveling past an ion, is determined by the Coulomb force and the time interval needed for the electron to pass the ion. The Coulomb force depends only on the relative distance between the two particles and is independent of the velocity of the electron. The time interval depends on the electron velocity, the higher the velocity of the electron, the smaller the time interval. Hence faster electrons are less collisional and experience a smaller friction force. Collisions with neutrals are not too dissimilar from collisions with ions, thus the higher the temperature, the lower the rate of collisional ionisation. However, the temperature change of 20 K was negligible compared to 100 eV (1.16 MK), which was the temperature of the electron, hence this could not be the cause of the decreasing voltage at higher temperature.

This would most likely be caused by the difference in pressure. But a higher pressure should have resulted in a higher offset voltage since the rate of collisional ionisation increased with pressure. This reversed behaviour could potentially be caused by the ionisation of a heavier element from the wall of the lens such as oxygen, introducing a different property to the plasma, decreasing the current measured at the detector. This requires further investigation via the use of an optical spectrometer, a distinct set of spectral lines would be observed if a different element was ionised due to their differences in energy levels.

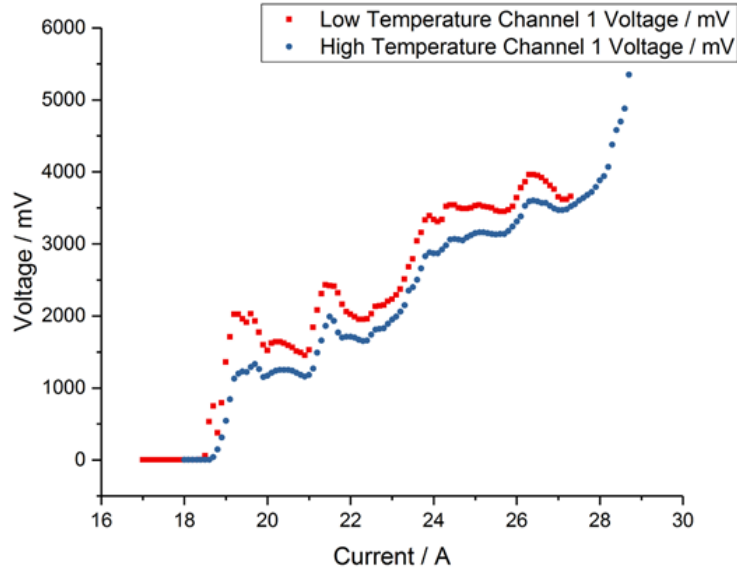


Figure 15: A graph showing how the offset voltage varied with the magnetic field produced by the current at 20 kV at different starting temperature of 22.2°C (red) and 38.6°C (Blue)

6.3.3 Variation in Current in the High Voltage supply

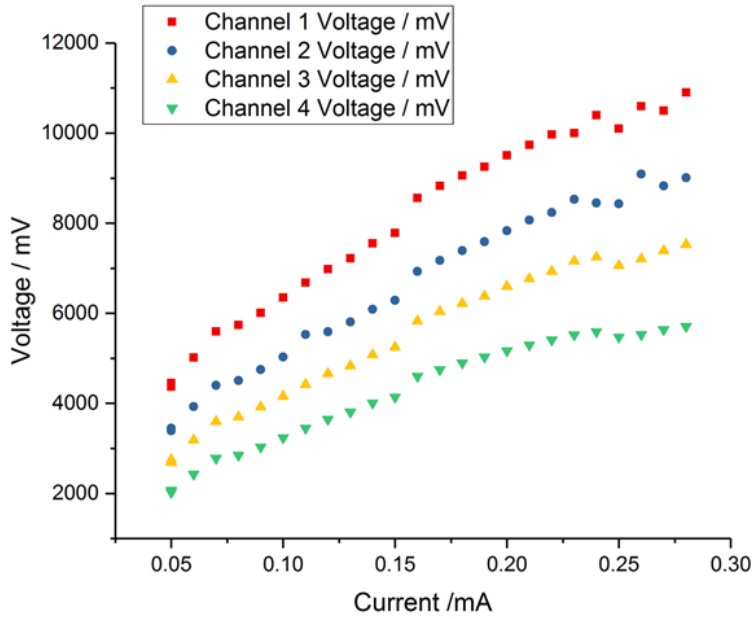


Figure 16: A graph showing how the offset voltage varied with the current at the HV supply in the limited current regime

This graph shows that the measured voltage increased with the current in the HV supply. This agreed with the results discussed in Section 3.3. As the current on the HV supply increased, the internal resistance of the HV supply increased, decreasing the voltage at the anode, hence the number of positive ions remained inside the chamber increased, increasing the density of the residual gas, thus increasing the current measured at the detector.

7 Problems Encountered

Initially, channel 3 measured zero voltage regardless of the conditions inside the lens. Each segment of the channel was then checked using a multimeter, and it was found that one of the segments were grounded. Voltages were measured in channel 3 after disconnecting the grounded segment. In order to compare the offset voltages between the channels, each one of the channels had one of its segments grounded.

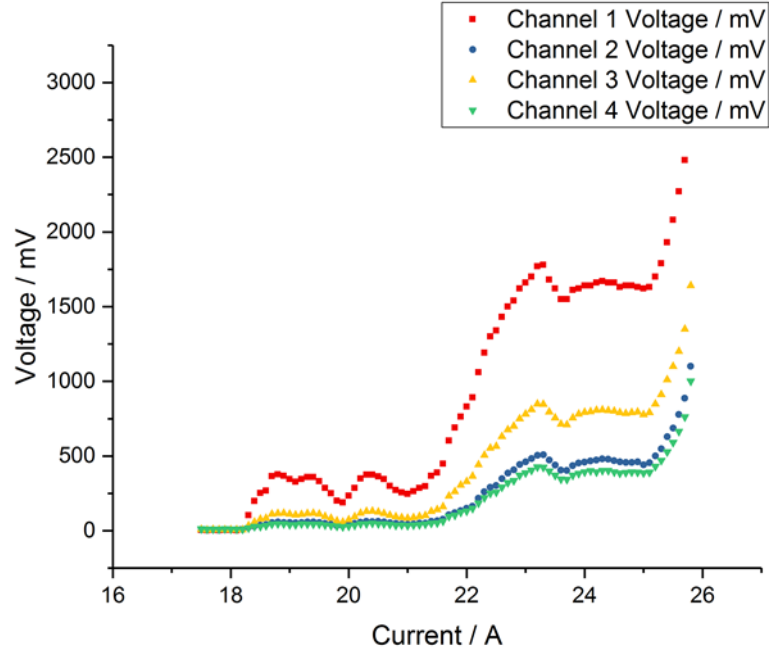


Figure 17: A graph showing how the offset voltage varied with the magnetic produced by the current at 12 kV with faulty connections

During the base voltage measurements, it was found that channel 2 measured a lower offset voltage than channel 3 shown in Figure 16, which was unexpected because channel 2 had a smaller radius than channel 3. Hence a complete check-up was done for every segment in the detector. Each segment was checked if it was grounded or connected to other segments, it was found that channel 1 and 3 each had one faulty segments, and channel 2 had two faulty segments. Since the problem of faulty wiring in the detector was so severe, it was decided that it was required to be fixed by resoldering the connections to the segments.

8 Conclusion and Outlook

The project was motivated by the de-focusing effect observed in the testing of the proton pencil beam in 2015, indicating that there were instabilities in the Gabor lens. The aim of the project was to investigate the causes and conditions of instabilities of the lens in different variable parameters including the magnetic field, high voltage supplied to the anode, temperature, and the location of the detector.

Different operating regimes were observed in the plasma and indicated that the voltage regime was the most favourable regime for the purpose of focusing due to its large Debye length. There were significant peaks observed below 220 Hz in the Fourier spectra of all three regimes, the exact cause of the peaks was yet to be determined, but it indicated that the relative amplitude of the peaks was correlated to the stability of the offset voltage. This could be further investigated by increasing the recording duration to increase the resolution of the Fourier spectrum, identifying the exact characteristic frequency of the peak and comparing with the frequency of the potential cause of the peak.

The experimental results of the mechanical movement of the detector mostly agreed with the simulation, verifying the theory for the production of positive ions and electrons. However, it indicated that the detector was not perfectly centred and slanted in the lens. The plasma unexpectedly operated in the current regime when the detector was shifted to the left, indicating that the detector was not perfectly grounded, and sparked between the grounded casing of the lens.

The temperature of the lens increased as the current flowed in the solenoid to produce the magnetic field, it was found that the offset voltage dropped as the temperature of the lens increased. This could be caused by the ionisation of a heavier element from the wall of the lens, decreasing the current at the detector. This could be further investigated by using an optical spectrometer, observing the sets of spectral lines to verify whether a different element was ionised.

Different features such as the failed attempts to form the plasma at non-Gabor conditions and the two plateau regions were observed in the base voltage measurements. The first plateau region was caused by the expulsion of the electrons, decreasing the positive ion current measured at the detector. The reason for the observation of the second plateau region was unknown, and the correlation between the HV and the offset voltage at the plateau region were masked. These could be caused by the change in temperature and could be verified by installing a cooling system in the lens.

In the near future, the Gabor lens will be tested with a laser-accelerated proton beam at the peak of the rapid rise before the plateau region as it was indicated to be the most stable and focusing in this project.

References

- [1] GABOR, D. (1947). A Space-Charge Lens for the Focusing of Ion Beams. *Nature*, 160(4055), pp.89-90.
- [2] Pozimski, J. (1992). First Experimental Studies of a Gabor-Plasma-Lens in Frankfurt.
- [3] Palkovic, J. (1988). Measurements on a Gabor Lens for Neutralizing and Focusing a 30 KeV Proton Beam. Linear Accelerator Conference.
- [4] Reiser, M. (1989). Comparison of Gabor Lens, Gas Focusing, and Electrostatic Quadrupole Focusing for Low-Energy Ion Beams.
- [5] Palkovic, J. (1989). Gabor Lens Focusing of A Negative Ion Beam.
- [6] wang, b. (2011). FP Generation fusion project was funded and built prototypes | NextBigFuture.com. [online] NextBigFuture.com. Available at: <http://www.nextbigfuture.com/2011/05/fp-generation-fusion-project-was-funded.html> [Accessed 2 Apr. 2017].
- [7] Enlight.web.cern.ch. (2017). What is Hadron Therapy? | The European Network for LIGHT ion Hadron Therapy. [online] Available at: <http://enlight.web.cern.ch/what-is-hadron-therapy> [Accessed 4 May 2017].
- [8] Global Vision, P. (2017). Proton Therapy Around the World - Proton Therapy Center, cancer treatment in Europe. [online] Proton-cancer-treatment.com. Available at: <http://www.proton-cancer-treatment.com/proton-therapy/proton-therapy-around-the-world/> [Accessed 4 May 2017].
- [9] Pozimski, J. (2012). Gabor Lens Focusing for Medical Applications.
- [10] Freeman, T. (2014). Gabor lens tailors laser-generated ion beams - MedicalPhysicsWeb. [online] Medicalphysicsweb.org. Available at: <http://medicalphysicsweb.org/cws/article/research/56348> [Accessed 3 Apr. 2017]
- [11] Posocco, P. (2016). First Test of the Imperial College Gabor (Plasma) Lens Prototype at the Surrey Ion Beam Centre.
- [12] Xia, Y. (2016). Analysis of the data collected during the 2015 experimental campaign.
- [13] Neuner, U. et al (2000). Shaping of Intense Ion Beams into Hollow Cylindrical Form. *Physical Review Letters*, 85(21), pp.4518-4521.
- [14] Pozimski, J. and Aslaninejad, M. (2013). Gabor lenses for capture and energy selection of laser driven ion beams in cancer treatment. *Laser and Particle Beams*, 31(04), pp.723-733.
- [15] Vacuum, P. (2017). Mean free path. [online] Pfeiffer-vacuum.com. Available at: <https://www.pfeiffer-vacuum.com/en/know-how/introduction-to-vacuum-technology/fundamentals/mean-free-path/> [Accessed 6 Apr. 2017].
- [16] Piero Possocco, Private Communication